



Cite this: *Chem. Commun.*, 2018, **54**, 5086

Received 1st March 2018,
Accepted 16th April 2018

DOI: 10.1039/c8cc01707g

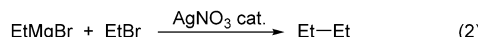
rsc.li/chemcomm

Despite the potential of silver to mediate synthetically valuable cross-coupling reactions, the operating mechanisms have remained unknown. Here, we use a combination of rapid-injection NMR spectroscopy, electrospray-ionization mass spectrometry, and quantum chemical calculations to demonstrate that these transformations involve argenate(I) and (III) complexes as key intermediates.

Organoargentates, unlike organocuprates, are not widely used in coupling reactions^{1,2} nor have they been as well characterized.^{3,4} This neglect is surprising given that early work demonstrated the potential of silver to mediate these transformations. Already in 1929, Gardner reported that reactions of Grignard reagents with stoichiometric amounts of silver salts gave rise to coupling reactions (eqn (1)).⁵ Over 40 years later Kochi demonstrated silver-catalyzed coupling (eqn (2)), and established that the mechanism is complex.⁶



R = Ph, *p*-MeC₆H₄, *p*-MeOC₆H₄, PhCH₂, *c*-C₆H₁₁, *n*-Bu



Since then there have been several other reports on silver-catalyzed coupling reactions,¹ but not much progress has been made in their mechanistic elucidation. In particular, the role of organoargentates(I) and organoargentates(III) in these reactions has received only little attention.^{4b,7–9} Here, we use a combination of:

^a Institut für Organische und Biomolekulare Chemie, Universität Göttingen, Tammannstraße 2, 37077 Göttingen, Germany.

E-mail: konrad.koszinowski@chemie.uni-goettingen.de

^b Department of Chemistry, University of North Carolina-Charlotte, Charlotte NC 28223, USA. E-mail: cogle@uncc.edu

^c School of Chemistry and Bio21 Molecular Science and Biotechnology Institute, University of Melbourne, 30 Flemington Rd, Parkville, Victoria 3010, Australia. E-mail: rohair@unimelb.edu.au

† Electronic supplementary information (ESI) available: Experimental and computational details, additional spectra, measured and theoretical *m/z* ratios, additional energy diagrams, calculated ΔG^{298} values. See DOI: [10.1039/c8cc01707g](https://doi.org/10.1039/c8cc01707g)

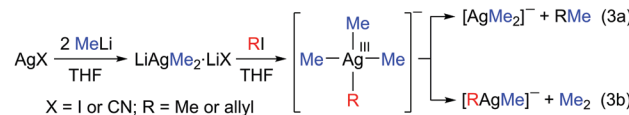
‡ These authors contributed equally.

Argenate(I) and (III) complexes as intermediates in silver-mediated cross-coupling reactions†

Sebastian Weske,‡^a Richard A. Hardin,‡^b Thomas Auth,‡^a Richard A. J. O'Hair, ID *^{ac} Konrad Koszinowski ID *^a and Craig A. Ogle ID *^b

(1) rapid-injection NMR spectroscopy¹⁰ and electrospray-ionization (ESI) mass spectrometry to show that organoargentates(III) are formed in reactions of alkyl iodides with dimethylargentate; (2) gas-phase experiments and quantum chemical calculations to examine the elementary step of reductive elimination from organoargentates(III).¹¹ The obtained mechanistic insight improves the fundamental understanding of the role of high-valent transition metals in cross-coupling reactions.¹²

Reaction of 2 equiv. of MeLi with silver(I) iodide at -78°C afforded the dimethylargentate LiAgMe₂·LiI (Scheme 1, X = I). Consistent with previous NMR-spectroscopic studies,^{3d} the ¹H NMR spectrum of LiAgMe₂·LiI in THF-*d*₈ at -100°C displayed a doublet at -1.25 ppm, which exhibited an averaged ²J_{Ag-H} coupling of 7.30 Hz (Fig. S1, ESI†), while the ¹³C NMR spectrum gave a chemical shift of -8.63 ppm, with ¹J_{109Ag-C} of 92.45 Hz and ¹J_{107Ag-C} of 83.69 Hz (Fig. S2, ESI†).§ Upon warming to -70°C , the dimethylargentate underwent an oxidative addition with allyl iodide (RI, 0.5 equiv.). The resulting transient intermediate [R(I)AgMe₂]⁻ was not detectable on the NMR time scale. Presumably, it immediately reacted with another equivalent of LiAgMe₂·LiI to displace iodide for a methyl group and produce the hitherto elusive tetraalkylargentate(III) complex [RAgMe₃]⁻ (Fig. 1) along with monomethylsilver. [RAgMe₃]⁻ slowly decomposed at -70°C to yield 1-butene *via* a reductive elimination (Scheme 1, eqn (3a)). The same product had also been observed for the reaction of LiCuMe₂·LiI and allyl chloride.^{10c} However, in that case the reactive organometallic species was not identified as the anionic ate complex, but the neutral intermediate [RCuMe₂]. Interestingly, we did not find an analogous [RAgMe₂] species in our present experiments.



Scheme 1 Formation of dimethylargentates LiAgMe₂·LiX and their subsequent reactions with methyl or allyl iodide.



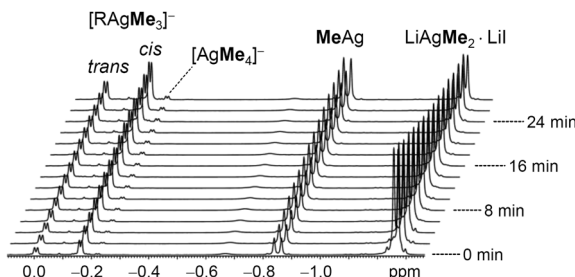


Fig. 1 Stacked plot of the high-field sections of the ^1H NMR spectra measured for the reaction of $\text{LiAgMe}_2\text{-LiI}$ with allyl iodide (RI) at $-70\text{ }^\circ\text{C}$ in $\text{THF-}d_8$.

In the ^1H NMR spectrum (Fig. S3–S6, ESI ‡), $[\text{RAgMe}_3]^-$ showed characteristic resonances at -0.01 and -0.16 ppm , which can be assigned to its Me_{trans} and Me_{cis} substituents, respectively. In both cases, averaged $^2J_{\text{Ag-H}}$ couplings of approx. 5 Hz were observed. Very similar behavior had previously been found for the related tretraalkylcuprate(III) $[\text{RCuMe}_3]^-$.^{10c} Further information could be obtained from the ^{13}C NMR spectrum of $[\text{RAgMe}_3]^-$ and, in particular, the $^1J_{\text{Ag-C}}$ coupling constants. With $^1J_{109\text{Ag-C}}$ and $^1J_{107\text{Ag-C}}$ couplings of 52.5 and 45.6 (Me_{trans}) and 48.9 and 42.4 Hz (Me_{cis}), respectively, the methyl groups of $[\text{RAgMe}_3]^-$ exhibited a smaller coupling to the silver nucleus than those in the dimethylargentate, in line with the expected change from sp to sp^2d hybridization.¹³ The α -allyl carbon in $[\text{RAgMe}_3]^-$ showed even smaller $^1J_{109\text{Ag-C}}$ and $^1J_{107\text{Ag-C}}$ couplings of 35.3 and 30.8 Hz , respectively, which point to a residual planarization in the allyl moiety and decreased s bonding character of the α -allyl carbon.

The reaction of $\text{LiAgMe}_2\text{-LiI}$ with allyl iodide also yielded small amounts of the tetramethylargentate(III) $[\text{AgMe}_4]^-$ (Fig. 1). Presumably, $[\text{AgMe}_4]^-$ originated from the substitution of the allyl group in $[\text{RAgMe}_3]^-$ by a methyl group from $\text{LiAgMe}_2\text{-LiI}$. $[\text{AgMe}_4]^-$ could also be prepared from $\text{LiAgMe}_2\text{-LiI}$ and MeI (Scheme 1), but only in poor yield. The synthesis was greatly improved by the addition of 2 equiv. of PMe_3 and the formation of neutral $[(\text{Me}_3\text{P})\text{AgMe}_3]$ (Fig. S7, ESI ‡), yielding $[\text{AgMe}_4]^-$ upon reaction with MeLi (Fig. S8, ESI ‡). $[\text{AgMe}_4]^-$ decomposed at temperatures above $0\text{ }^\circ\text{C}$ and showed ^1H and ^{13}C NMR resonances and coupling constants much alike those of the methyl groups of its heteroleptic congener $[\text{RAgMe}_3]^-$. In contrast to the latter, $[\text{AgMe}_4]^-$ gave only one set of signals, thus reflecting its higher symmetry. Moreover, its ^1H NMR-spectroscopic signature closely resembles that of its $[\text{CuMe}_4]^-$ homologue.^{10d}

Next, we turned to negative-ion mode electrospray-ionization (ESI) mass spectrometry to analyze a THF solution of $\text{LiAgMe}_2\text{-Li}(\text{CN})$. We observed a series of ate complexes including $[\text{Ag}_n\text{Me}_{n+1}]^-$ ($n = 2\text{--}4$), $[\text{Li}_2\text{Ag}_3\text{Me}_6]^-$, and $[\text{LiAg}_2\text{Me}_{4-n}(\text{CN})_n]^-$ ($n = 1, 2$), but no significant amounts of mononuclear $[\text{AgMe}_2]^-$ (Fig. S9, ESI ‡).^{8¶}¹⁴ These assignments were confirmed by both the accurate mass measurements (Table S1, ESI ‡) as well as the isotope patterns (Fig. S10–S26, ESI ‡). Organocuprates give similar ESI mass spectra.¹⁵ Most likely, the predominance of polynuclear ions in the mass-spectrometric experiments results from the shift of aggregation equilibria during the ESI process.^{15c,16} Upon the addition of methyl or allyl iodide, the spectra changed markedly

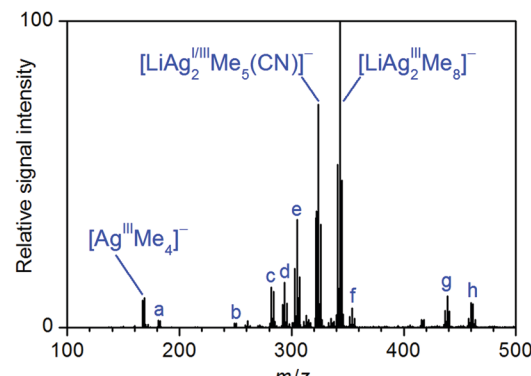


Fig. 2 Negative-ion mode ESI mass spectrum of the products formed upon reaction of $\text{LiAgMe}_2\text{-Li}(\text{CN})$ with methyl iodide (0.5 equiv.) in THF (concentration of the argenteate in the sample solution: 25 mM). (a): $[\text{LiAg}^1\text{Me}(\text{CN})]^-$, (b): $[\text{Ag}^3\text{Me}]^-$, (c): $[\text{LiAg}^1\text{Me}(\text{CN})]^-$, (d): $[\text{LiAg}_2^1\text{Me}_3(\text{CN})]^-$ and $[\text{LiAg}_2^1\text{Me}_2(\text{OH})(\text{CN})]^-$, (e): $[\text{LiAg}_2^1\text{Me}_2(\text{CN})_2]^-$, (f): $[\text{LiAg}_2^1\text{Me}_7(\text{CN})]^-$, (g): $[\text{Li}_2\text{Ag}_2^1\text{Me}_2(\text{CN})_2]^-$, (h): $[\text{Li}_2\text{Ag}_3^1\text{Me}_3(\text{CN})_3]^-$.

and showed mononuclear Ag(III) ate anions as well as the corresponding higher aggregates as new species. The reaction with MeI afforded the lithium-bound dimer $[\text{LiAg}_2\text{Me}_6]^-$ as base peak (Fig. 2 and Fig. S20–S26, ESI ‡). The same ion as well as the related heteroleptic species $[\text{LiRAg}_2\text{Me}_7]^-$ and $[\text{LiR}_2\text{Ag}_2\text{Me}_6]^-$ were observed for the reaction with allyl iodide (RI, Fig. S27–S32, ESI ‡). Argenteate(III) complexes were also observed in control experiments with cyclopentyl methyl ether or *tert*-butyl methyl ether as solvents (Fig. S33–S39, ESI ‡).

The gas-phase fragmentation of the mass-selected homoleptic mononuclear complex $[\text{AgMe}_4]^-$ solely led to the reductive elimination of ethane (Fig. S40, ESI ‡).[§] Its heteroleptic counterpart $[\text{RAgMe}_3]^-$ also underwent reductive elimination (Fig. 3) and preferentially released the cross-coupling product RMe (eqn (3a)), whereas the homo-coupling product Me_2 (eqn (3b)) was formed only to a much smaller extent (Fig. 3). This result is consistent with the solution-phase NMR experiment, but is in stark contrast with gas-phase fragmentation of the related allylcuprate, $[\text{RCuMe}_3]^-$, for which the dominant channel affords the homo-coupling product.^{15c} This finding for the first time shows that silver-mediated cross-coupling may substantially differ from the

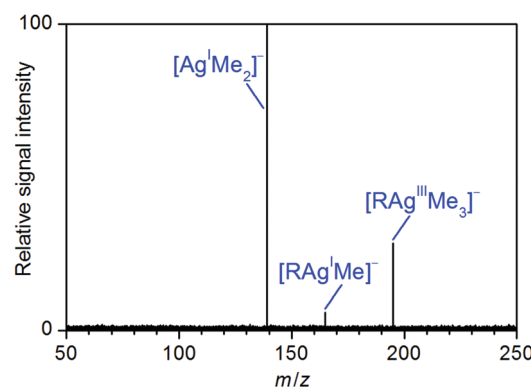
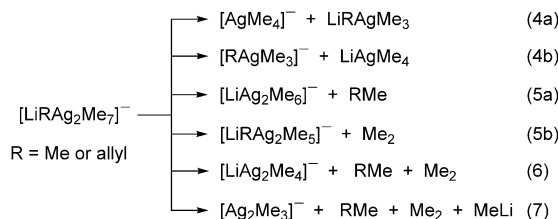


Fig. 3 Mass spectrum of mass-selected $[\text{R}^{107}\text{AgMe}_3]^-$ ($m/z 193$) and its fragment ions produced upon collision-induced dissociation at $E_{\text{LAB}} = 7.5\text{ eV}$.

corresponding copper-based reactions. Fragmentation of the lithium-bound dimers resulted in formation of the mononuclear complexes (eqn (4)) and reductive eliminations (eqn (5), Fig. S41–S43, ESI†). For the heteroleptic complexes, cross-coupling (eqn (5a)) again strongly prevailed over homo-coupling (eqn (5b)). Secondary fragmentation reactions were also observed (eqn (6) and (7)).



To obtain further insight into the reductive elimination as the product-forming step, we carried out quantum chemical calculations. The exothermic release of ethane from $[\text{AgMe}_4]^-$ proceeds *via* a C_2 -symmetric transition structure, which is predicted to be 166 kJ mol⁻¹ higher in energy than the reactant (Fig. 4). The resulting ion–molecule complex easily dissociates into $[\text{AgMe}_2]^-$ and the coupling product. According to a natural population analysis (NPA),¹⁷ the release of ethane is accompanied by a decrease of the charge of the silver center from 0.56 to 0.25 (Fig. 4), consistent with a reduction from Ag(III) to Ag(I).^{18,19} For the lithium-bound dimer $[\text{LiAg}_2\text{Me}_8]^-$ the energy of the transition structure associated with the reductive elimination of ethane is calculated at 127 kJ mol⁻¹ (Fig. S44, ESI†), a value significantly lower than for the mononuclear complex. Apparently, the interaction with the lithium center lowers the barrier substantially. This effect can be rationalized by Li^+ withdrawing electron density from the ate complex and thereby raising the propensity of the silver(III) center to regain its preferred oxidation state of +I by reductive elimination. A similar trend has been found for the corresponding cuprate(II) complexes $[\text{CuMe}_4]^-$ and $[\text{LiCu}_2\text{Me}_8]^-$.^{15c} The competing dissociation of $[\text{LiAg}_2\text{Me}_8]^-$, eqn (4), requires an energy of 173 kJ mol⁻¹ and, thus, is energetically more demanding than the reductive elimination. However, the latter reaction is

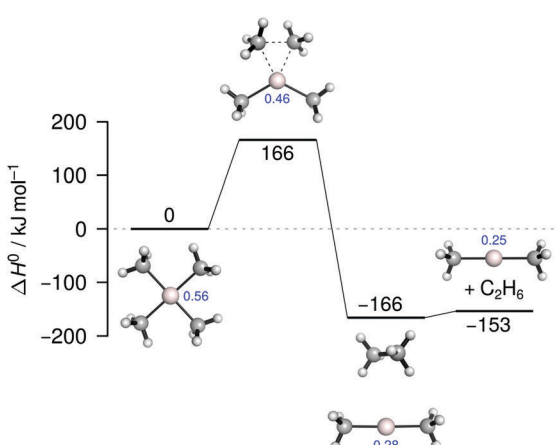


Fig. 4 Energy diagram for the gas-phase reductive elimination of ethane from $[\text{AgMe}_4]^-$ obtained from quantum chemical calculations. NPA charges of Ag are shown in blue.

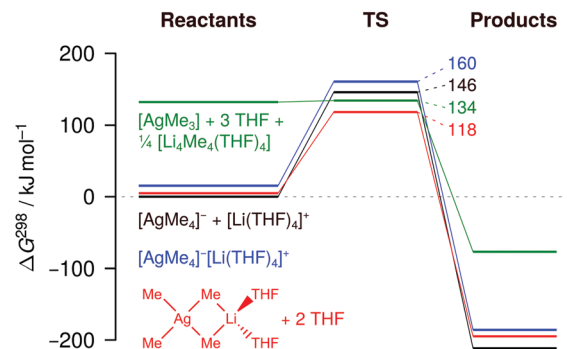


Fig. 5 Energy diagram for the reductive elimination of ethane from: free ions (black); solvent separated ion pair (blue); contact-ion pair (red); neutral $[\text{AgMe}_3]$ (green) in THF obtained from quantum chemical calculations.

entropically favored (Fig. S44, ESI†), which explains why it is found to compete with the former in the experiment (Fig. S41, ESI†). Thus, the results of the quantum chemical calculations are in full accordance with those of the gas-phase fragmentation experiments.

We also used theoretical methods to investigate the occurrence of reductive eliminations from $[\text{AgMe}_4]^-$ and related systems in THF. Apart from the free ions, we considered solvent-separated and contact-ion pairs (Fig. 5, Fig. S45 and Table S2, ESI†). Our calculations predict that ion pairing does not strongly affect the Gibbs energy of the reactant argenate(III) complex at 298 K, but that the interaction with Li^+ in the contact-ion pair substantially stabilizes the transition state, thus facilitating the overall reaction. This reactivity-enhancing effect of lithium essentially equals that already found for the gaseous $[\text{LiAg}_2\text{Me}_8]^-$ complex discussed above. For comparison, we also included the neutral species AgMe_3 in our analysis, taking into account that the formation of this species from $[\text{AgMe}_4]^-[\text{Li}(\text{THF})_4]^+$ generates 0.25 equiv. of $[\text{Li}_4\text{Me}_4(\text{THF})_4]$ as the most stable form of MeLi in THF (Fig. 5; for the reactivity of other neutral systems, see Fig. S46, ESI†).²⁰ Similar to previous theoretical results of Nakamura and coworkers, we find AgMe_3 to eliminate ethane without any significant barrier.⁸ Nevertheless, the overall reaction proceeding *via* neutral $[\text{AgMe}_3]$ is still less favorable than the reaction *via* the contact-ion pair because the formation of $[\text{AgMe}_3]$ requires a large amount of energy. Thus, our calculations indicate that silver-mediated C–C coupling in solution indeed involves argenate complexes as central intermediates, whose reactivity is strongly influenced by Li^+ counter-ion effects.

In conclusion, we have shown that Ag(I) and Ag(III) ate complexes are crucial intermediates in C–C coupling. Remarkably, the silver-mediated coupling reactions with allyl halides differed significantly from the previously studied copper-mediated reactions. For copper, the cross-coupling product evolves from the neutral allyl-containing intermediate $[\text{RCuMe}_2]$. In contrast, we did not observe the analogous silver complex in the present experiments. This finding suggests that the silver-mediated formation of the cross-coupling product proceeds from anionic Ag(III) ate complexes. Our gas-phase experiments directly show the feasibility of this reaction. This mode of reactivity deviates from that of the analogous cuprate, which preferentially affords the homo-coupling instead of the cross-coupling product. Preliminary quantum chemical



calculations on the competition between the reductive elimination elementary steps for isolated $[\text{R}\text{AgMe}_3]^-$ and $[\text{RCuMe}_3]^-$ anions reveal that fundamentally different mechanisms operate. Clearly, organoargentates are more than just a costly variant of the all popular organocuprates. The improved understanding of their mode of action also promises to boost their use in synthesis.

S. W., T. A., and K. K. gratefully acknowledge support from the DFG (KO 2875/6-1). R. A. J. O. thanks the Humboldt foundation for the award of a senior fellowship.

Conflicts of interest

There are no conflicts to declare.

References

- Rapid-injection NMR experiments were carried out as previously described.¹⁰ For the mass-spectrometric experiments, sample solutions were injected (flow rate of 8 $\mu\text{L min}^{-1}$) into the ESI source (ESI voltage of 3.5 kV, N_2 as nebulizer and dry gas, 60 °C) of a micrOTOF-Q II mass spectrometer (Bruker Daltonik). In gas-phase fragmentation experiments, ions were mass-selected (isolation width of 1.0–2.0 u), accelerated to a kinetic energy of E_{LAB} , and allowed to collide with N_2 gas. Molecular structures were obtained by PBE0-D3BJ²¹ geometry optimizations. For all structures, DLPNO-CCSD(T)²² single-point energies (SPEs) were calculated. To determine G^{298} values in THF, solvation energies ΔG_{solv} were calculated for each structure as difference between the PBE0-D3BJ SPE and the SPE obtained from a C-PCM²³ PBE0-D3BJ calculation. Additional SMD²⁴ PBE0-D3BJ calculations of ΔG_{solv} support the validity of the ΔG^{298} (C-PCM) results (Fig. S47 and Table S2, ESI[†]). For further details, see the ESI.[†]
- Control experiments showed that both $\text{Ag}(\text{CN})$ and AgI afforded similar ESI mass spectra upon reaction with MeLi . The sample solutions formed from $\text{Ag}(\text{CN})$ were more stable and directly comparable to those formed from $\text{Cu}(\text{CN})$ reported in ref. 15c.
- Reviews on organosilver chemistry: (a) J.-M. Weibel, A. Blanc and P. Pale, *Chem. Rev.*, 2008, **108**, 3149; (b) *Silver in Organic Chemistry*, ed. M. Harmata, Wiley, Hoboken, 2010; (c) J. Cossy, in *Grignard Reagents and Transition Metal Catalysts*, ed. J. Cossy, Walter de Gruyter, Berlin/Boston, 2016, ch. 7.
- Reviews on organocuprate chemistry: (a) R. M. Gschwind, *Chem. Rev.*, 2008, **108**, 3029; (b) *The Chemistry of Organocuppper Compounds*, ed. Z. Rappoport, I. Marek, Wiley, Hoboken, 2009; (c) N. Yoshikai and E. Nakamura, *Chem. Rev.*, 2012, **112**, 2339.
- For argentates(i), see: (a) C. Eaborn, P. B. Hitchcock, J. D. Smith and A. C. Sullivan, *J. Chem. Soc., Chem. Commun.*, 1984, 870; (b) M. Y. Chiang, E. Böhlen and R. Bau, *J. Am. Chem. Soc.*, 1985, **107**, 1679; (c) R. R. Burch and J. C. Calabrese, *J. Am. Chem. Soc.*, 1986, **108**, 5359; (d) D. E. Bergbreiter, T. J. Lynch and S. Shimazu, *Organometallics*, 1983, **2**, 1354.
- For stable isolated argentates(ii) bearing fluorinated organyl substituents, see: (a) W. Dukat and D. Naumann, *Rev. Chim. Miner.*, 1986, **23**, 589; (b) R. Eijken, B. Hoge and D. J. Brauer, *Inorg. Chem.*, 1997, **36**, 1464; (c) R. Eijken, B. Hoge and D. J. Brauer, *Inorg. Chem.*, 1997, **36**, 3160.
- H. Gardner and P. Borgstrom, *J. Am. Chem. Soc.*, 1929, **51**, 3375.
- K. Kochi and M. Tamura, *J. Am. Chem. Soc.*, 1971, **93**, 1483.
- K. Murakami, K. Hirano, K. Yorimitsu and K. Oshima, *Angew. Chem., Int. Ed.*, 2008, **47**, 5833.
- For theoretical studies on silver-mediated carbon–carbon coupling reactions, see: W. Nakanishi, M. Yamanaka and E. Nakamura, *J. Am. Chem. Soc.*, 2005, **127**, 1446.
- Cationic $\text{Ag}(\text{III})$ complexes have recently been demonstrated to be involved in catalytic cross-coupling reactions: M. Font, F. Acuña-Parés, T. Parella, J. Serra, J. M. Luis, J. Lloret-Fillol, M. Costas and X. Ribas, *Nat. Commun.*, 2014, **5**, 4373.
- (a) S. H. Bertz, S. Cope, M. Murphy, C. A. Ogle and B. J. Taylor, *J. Am. Chem. Soc.*, 2007, **129**, 7208; (b) S. H. Bertz, S. Cope, D. Dorton, M. Murphy and C. A. Ogle, *Angew. Chem., Int. Ed.*, 2007, **46**, 7082; (c) E. R. Bartholomew, S. H. Bertz, S. Cope, M. Murphy and C. A. Ogle, *J. Am. Chem. Soc.*, 2008, **130**, 11244; (d) E. R. Bartholomew, S. H. Bertz, S. K. Cope, M. D. Murphy, C. A. Ogle and A. A. Thomas, *Chem. Commun.*, 2010, **46**, 1253.
- For gas-phase studies on the reductive elimination of other high-valent transition-metal complexes, see: (a) K. L. Vikse, M. A. Henderson, A. G. Oliver and J. S. McIndoe, *Chem. Commun.*, 2010, **46**, 7412; (b) J. Hývl and J. Roithová, *Org. Lett.*, 2014, **16**, 200; (c) E. P. A. Couzijn, I. J. Kobylanski, M.-E. Moret and P. Chen, *Organometallics*, 2014, **33**, 2889.
- J. Hickman and M. S. Sanford, *Nature*, 2012, **484**, 177.
- J^1 coupling constants correlate with the s character of the binding electrons: R. K. Harris, *Nuclear Magnetic Resonance Spectroscopy*, Longman Science & Technical, Essex, 1986.
- Organogold(I)argentates have been prepared in the gas-phase via de-carboxylation and their reactivity has been examined: (a) R. A. J. O'Hair, *Chem. Commun.*, 2002, 20; (b) N. J. Rijs and R. A. J. O'Hair, *Organometallics*, 2010, **29**, 2282; (c) N. J. Rijs, N. Yoshikai, E. Nakamura and R. A. J. O'Hair, *J. Am. Chem. Soc.*, 2012, **134**, 2569.
- (a) A. Putau and K. Koszinowski, *Organometallics*, 2010, **29**, 3593; addition/correction: A. Putau and K. Koszinowski, *Organometallics*, 2010, **29**, 6841; (b) A. Putau and K. Koszinowski, *Organometallics*, 2011, **30**, 4771; (c) A. Putau, H. Brand and K. Koszinowski, *J. Am. Chem. Soc.*, 2012, **134**, 613.
- The nanodroplets formed in the ESI process constantly lose solvent molecules due to evaporation and, thus, become enriched in the analyte, see: (a) A. Wortmann, A. Kistler-Momotova, R. Zenobi, M. C. Heine, O. Wilhelm and S. E. Pratsinis, *J. Am. Soc. Mass Spectrom.*, 2007, **18**, 385; (b) N. G. Tsierkezos, J. Roithová, D. Schröder, M. Ončák and P. Slavíček, *Inorg. Chem.*, 2009, **48**, 6287.
- E. Reed, R. B. Weinstock and F. Weinhold, *J. Chem. Phys.*, 1985, **83**, 735.
- Calculated partial charges are well-known to deviate from formal oxidation states: (a) G. Aullón and S. Alvarez, *Theor. Chem. Acc.*, 2009, **123**, 67; (b) P. Karen, *Angew. Chem., Int. Ed.*, 2015, **54**, 4716.
- For a discussion about the oxidation states of related $\text{Cu}(\text{III})$ species, see: R. Hoffmann, S. Alvarez, C. Mealli, A. Falceto, T. J. Cahill III, T. Zeng and G. Manca, *Chem. Rev.*, 2016, **116**, 8173.
- A. Ogle, B. K. Huckabee, H. C. Johnson IV, P. F. Sims, S. D. Winslow and A. A. Pinkerton, *Organometallics*, 1993, **12**, 1960.
- (a) C. Adamo and V. Barone, *J. Chem. Phys.*, 1999, **110**, 6158; (b) S. Grimme, S. Ehrlich and L. Goerigk, *J. Comput. Chem.*, 2011, **32**, 1456.
- C. Riplinger, P. Pinski, U. Becker, E. F. Valeev and F. Neese, *J. Chem. Phys.*, 2016, **144**, 024109.
- V. Barone and M. Cossi, *J. Phys. Chem. A*, 1998, **102**, 1995.
- A. V. Marenich, C. J. Cramer and D. G. Truhlar, *J. Phys. Chem. B*, 2009, **113**, 6378.

